CHAPTER 7

Metal-Ligand Bonding:

❖ Limitation of Crystal Field Theory

The main drawback of the crystal field theory is that it does not consider the covalent character in metal-ligand bonding at all. It treats the metal-ligand interaction in a purely electrostatic framework which is pretty far from reality. All the effects which originate from covalence cannot be explained by this theory. Therefore, the main limitations of crystal field theory can be concluded only after knowing the causes and magnitude of the covalence in the metal-ligand bonds.

➢ *Evidences for the Covalent Character in Metal–Ligand Bond*

The crystal field theory considers the metal center as well as surrounding ligands as point charges and assumes that the interaction between them is 100% ionic. However, quite strong experimental evidences have proved that there is some covalent character too which cannot be ignored. Some of those experimental evidences are as follows:

1. The nephelauxetic effect: The electrons present in the partially filled *d*-orbitals of the metal center repel each other to produce a number of energy levels. The placement of these levels on the energy scale depends upon the arrangement of filled electrons. The energy of these levels can be given in terms of "Racah parameters" *B* and *C* (a measure of interelectronic repulsion). The energy difference between same multiplicity states is expressed in *B* and *Dq* while between different multiplicity states is given in term of *B*, *Dq* and *C*. It has been observed that the complexation of metal center always results in a decrease in interelectronic repulsion parameters which in turn also advocates a decrease in the repulsion between *d*-electron density. Now, as the magnitude of this interelectronic repulsion is dependent upon the distance between the areas of maximum charge density, the decrease in its value is expected only when the *d*-orbital lobes extend in space. This is called as the nephelauxetic effect and measured as the nephelauxetic parameter (β).

This extension or nephelauxetic effect may be attributed to the larger orbital overlap between metal and ligand resulting in greater stabilization due to covalent bonding. Hence, the direct effect of covalent bonding between metal and ligand is to decrease the interelectronic repulsion parameters. In other words, greater the decrease in "Racah parameters", larger is the extent of covalent bonding between metal and ligand. Different ligands have different capacity to extend their *d*-orbital and are arranged in ascending order, known as the nephelauxetic series as:

$$F^- < H_2O < NH_3 < Ox^{2-} < en < NCS^- < Cl^- < CN^- < Br^- < I^-$$

It has been observed that the nephelauxetic ratio always follows a certain trend with respect to the nature of the ligands present. However, there are many ligands that do not form complexes with a particular metal ion; the Racah parameter and for these complexes cannot be calculated empirical rather experimentally.

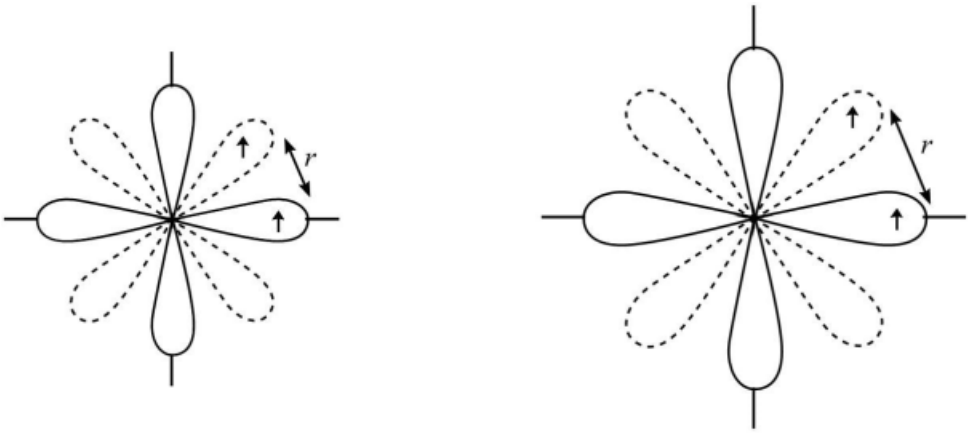

Figure 1. The expansion of *d*-electron cloud in transition metal centre after complexation due to nephelauxetic effect.

Hence, the observed decrease in inter-electronic repulsion parameters after complexation proves that there is always a somewhat more or less covalent character in the metal-ligand bond.

2. Lande's splitting factor: The value of Lande's splitting factor or simply "*g*-factor" for transition metal complexes was found to be different from what was expected from a pure ionic bonding perspective. The experimental value of *g*-factor showed that the electron from metal ion is always somewhat more or less delocalized to the ligand orbitals. This is possible only if metal orbitals are in overlap with the ligand orbitals via covalent interaction. Therefore, in view of the observed value of *g*-factor, we can claim that the partial covalence does exist in the metal-ligand bond.

3. Electron spin resonance spectra: It has been observed that the electron paramagnetic resonance or EPR spectra of some metal complexes is not that simple as expected. The fine lines were further split into hyperfine lines due to NMR active nuclei of ligands. This result can be explained only if the unpaired electrons of the metal center are delocalized to the nuclei centers of the ligands and as a consequence, electron-nucleus coupling occurs. Therefore, it quite obvious that we consider the metal-ligand as somewhat more or less covalent in nature. For example, the electron-spin resonance spectra of $[Ir(Cl_6)]^{2-}$ revealed that the unpaired 5*d*-electron of Ir^{4+} spends 70% of its time on Ir^{4+} while 30% on chloride ligands.

4. Nuclear magnetic resonance spectra: The nuclear magnetic resonance of some ligands in metal complexes is markedly affected by the unpaired electrons of the metal center. This is possible only if metal orbitals are in overlap with the ligand orbitals. This proves a covalence in metal-ligand bond. For example, the chemical shift of tris-(acetylacetonato) vanadium(III) is shifted towards a position as if there is no paramagnetic contribution from the metal ion. This anomaly in the chemical shift may be attributed to the transfer of unpaired electron density from vanadium ion to the attached ligand.

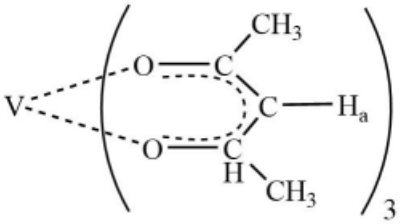

Furthermore, the F^{19} NMR of metal-fluoride complexes shows a significant effect arising from the unpaired electron from the metal centers, which obviously suggests that the electron on transition metal center does spend a non-zero time on the ligand too.

5. Nuclear quadrupole resonance: The nuclear quadrupole resonance spectra of some metal complexes having halide ions as ligands showed that the metal-halogen bond is not 100% ionic but has some covalent character too. In general, higher the NQR frequencies are, the larger will be the covalent character in metal-ligand bond. For example, one of the orders of the covalent character provided by nuclear quadrupole studies is Hg–X >> Cd–X > Zn–X, which is also supported by the Hard-Soft Acid-Base principal.

6. Kramers-Anderson superexchange: The phenomenon of superexchange was first suggested by H. Kramers in 1934 when he observed that in some crystals such as MnO, the Mn atoms interact with each another despite having diamagnetic intermediates like the oxide ions between them. Later on, Phillip Anderson modified the Kramers' model in the years of 1950. The superexchange phenomenon is the strong antiferromagnetic interaction between two nearest neighboring cations via a non-magnetic intermediate. Therefore, it is different from the direct-exchange in which the interaction is between nearest-neighbor cations without involving an intermediate anion.

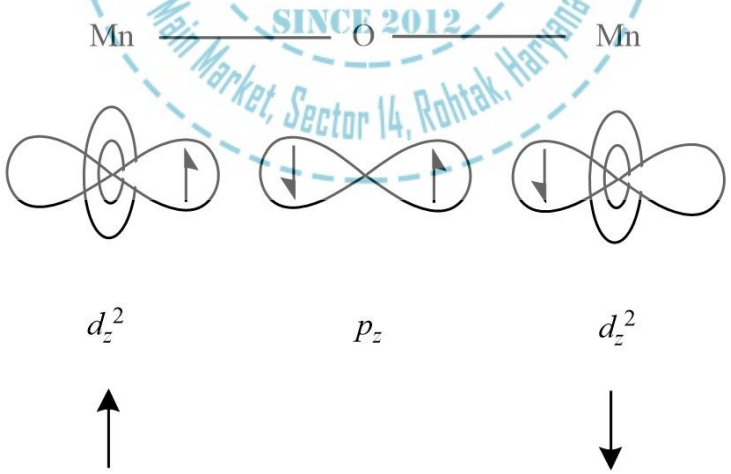

Figure 2. The superexchange phenomenon in MnO.

However, it may also be worthy to mention that if two neighboring cations are joined at 90 degrees to the diamagnetic bridge, then the coupling can be ferromagnetic in nature.

The phenomenon of superexchange can be rationalized with the help of Pauli exclusion principle which governs that the superexchange would lead to anti-ferromagnetic behavior if the coupling occurs between two ions each of which has half-filled orbital; and would yield ferromagnetic behavior one metal ion is having half-filled orbital while the other ion has fully-filled orbitals; provided that in both cases, they interact via a diamagnetic intermediate like O^{2-}. Moreover, the interaction between an ion with either filled or a half-filled orbital and one with an empty orbital can be either ferromagnetic or antiferromagnetic, however, it usually favors ferromagnetism. However, if multiple kinds of interactions are simultaneously present, the antiferromagnetic ordering is the one that usually dominates because of its independence of the intra-atomic exchange term. The whole of the above explanation is based on the fact that the bonding between the metal center and ligand is not 100% ionic but does have a significant extant of orbital-overlap which confirms the presence of covalent character.

- ***Limitations of CFT***

Now as we have discussed the covalence in metal-ligand bond, the main limitations of the crystal field theory can be summarized as follows:

1. The predictions of crystal field theory deviate from experimental results more and more as the extent of covalence between the metal center and ligands increases.

2. This theory does not give any satisfactory explanation for the relative strength of different ligands and hence is unable to explain the trends in the spectrochemical series. For example, ionic ligands are expected to show greater splitting effect due to the assumption of ligands as point charges but the neutral ligands like NH_3 or H_2O are actually stronger ligands than that of halide ions.

3. The crystal field theory gives no insight of back-bonding between the metal and ligand and fails to explain the π-bonding or multiple bonds.

4. It does not explain the charge-transfer bands observed in the UV-visible spectra of transition complexes.

5. The crystal field theory considers only the *d*-orbitals of central metal ion but takes no account of the *s* and *p*-orbitals for its calculations.

6. The crystal field theory does not consider the orbitals of ligands at all and hence does not explain any properties associated with ligand orbitals and their interaction with orbitals of the metal center.

7. The assumption of the interaction between metal and ligand as purely electrostatic in nature is an idealistic one and is pretty far from reality.

8. This theory does not explain the effect of π-bonding on crystal field splitting Δ and therefore cannot compare the π-acid characters.

9. It could not explain the color the metal complexes having full or empty *d*-orbitals.

10. The CFT overlooks the attractive forces acting between the *d*-electrons of the metal center and nuclear charge on the ligands attached, which results in an unclear image of the properties dependent upon the same.

❖ Molecular Orbital Theory – Octahedral, Tetrahedral or Square Planar Complexes

The crystal field theory fails to explain many physical properties of the transition metal complexes because it does not consider the interaction between the metal and ligand orbitals. The molecular orbital theory can be very well applied to transition metal complexes to rationalize the covalent as well as the ionic character in the metal-ligand bond. A transition metal ion has nine valence atomic orbitals which are consisted of five *nd*, three (n+1)*p*, and one (n+1)*s* orbitals. These orbitals are of appropriate energy to form bonding interaction with ligands. The molecular orbital theory is highly dependent on the geometry of the complex and can successfully be used for describing octahedral complexes, tetrahedral and square-planar complexes. The main features of molecular orbital theory for metal complexes are as follows:

1. The atomic orbital of the metal center and of surrounding ligands combine to form new orbitals, known as molecular orbitals.

2. The number of molecular orbitals formed is the same as that of the number of atomic orbitals combined.

3. The additive overlap results in the bonding molecular orbital while the subtractive overlap results in the antibonding overlap.

4. The energy of bonding molecular orbitals is lower than their nonbonding counterparts while the energy of antibonding molecular orbitals is higher than that of nonbonding orbitals.

5. The energy of nonbonding orbitals remains the same.

6. The ionic character of the covalent bond arises from the difference in the energy of combining orbitals.

7. If the energy of a molecular orbital is comparable to an atomic orbital, it will not be very much different in nature from atomic orbital.

The polarity of the bond can be explained by considering the overlap of two atomic orbitals of different energies. Suppose ϕ_A and ϕ_B are two atomic orbitals of atoms A and B, respectively. These two atomic orbitals have one electron in each of them and combine to form one bonding (σ) and one antibonding (σ^*) molecular orbital. After the formation of molecular orbitals, both electrons occupy σ-orbital. Now, if the energy of σ-orbital is closer to ϕ_A, it will have more ϕ_A character and hence the electron density of both of the electrons will be concentrated more on atom A than B. Similarly if the energy of σ-orbital is closer to ϕ_B, it will have more ϕ_B character and the electron density of both of the electrons will be concentrated more on atom B than A. This same explanation holds for the ionic character in metal-ligand bond.

The main concern here is that the total number of the molecular orbitals formed as a result of bonding and antibonding interactions is quite large; and therefore, many complications related to the understanding of symmetry-energy may arise, all of which needs a very sophisticated treatment of chemical bonding. Hence, without a comprehensive knowledge of the chemical applications of group theory, it is quite difficult to explain the whole concept. However, a primitive explanation for the σ-bonding in transition metal complexes of different geometry can still be given.

➢ *Octahedral Complexes*

In octahedral complexes, the molecular orbitals created by the coordination of metal center can be seen as resulting from the donation of two electrons by each of six σ-donor ligands to the *d*-orbitals on the metal. The metal orbitals taking part in this type of bonding are *nd*, $(n+1)p$ and $(n+1)s$. It should be noted down that not all *nd*-orbitals but only d_z^2 and $d_{x^2-y^2}$ orbitals are capable of participating in the σ-overlap. The d_{xy}, d_{xz} and d_{yz} orbitals remain non-bonding orbitals. The ligands approach the metal center along the *x*, *y* and *z*-axes in such a way that their σ-symmetry orbitals form bonding and anti-bonding combinations with metal's *s*, p_x, p_y, p_z, d_z^2 and $d_{x^2-y^2}$ orbitals. A total of six bonding and six anti-bonding molecular orbitals formed. The symmetry designations of different metal orbitals taking part in octahedral overlap are:

d_z^2, $d_{x^2-y^2}$	–	e_g
s	–	a_{1g}
p_x, p_y, p_z	–	t_{1u}
d_{xy}, d_{xz}, d_{yz}	–	t_{2g}

The exact nature of the Mulliken symbols, like e_g or a_{1g} etc., can be understood only after the core level understanding of group theory. However, it still can be noted that *a*, *e* and *t* represents singly, doubly and triply degenerate orbitals, respectively. The subscripts *g* and *u* represent gerade and ungerade nature of the orbitals. An orbital is said to be gerade if it has the same sign in all opposite directions from the center. These are also said to be having the centre of symmetry. On the other hand, an orbital is said to be ungerade if it has the opposite sign in all the opposite directions from the center. These are also said to be lacking the centre of symmetry.

The symmetry adapted linear combinations of atomic orbitals (SALCs) for metal-ligand direct overlap can be obtained just by resolving the reducible representation based on the bond vectors along the axis of σ-overlap. As there are total six bond vectors for the metal-ligand σ-bonding, hexa-dimensional reducible representation will be obtained. As the six ligands in an octahedral complex approach the central metal ion along the three Cartesian axes (two along *x*-axis, two along *y*-axis and two along *z*-axis), the six σ-basis bond vectors must also be selected along *x*, *y* and *z*-axis.

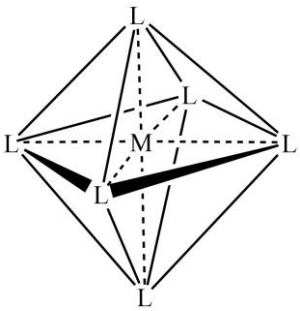

Figure 3. Continued on the next page…

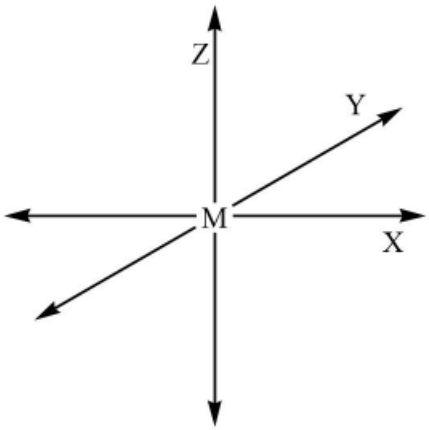

Figure 3. The octahedral coordination and corresponding σ-basis set for ligand orbitals in octahedral complexes.

The symmetry adapted linear combinations of these fall into three irreducible representations labeled as a_{1g}, e_g, and t_{1u}. The symmetry designations of different ligand orbitals taking part in octahedral overlap are:

Table 1. Reducible representation based on bond vectors in the octahedral geometry.

O_h	E	$8C_3$	$6C_2$	$6C_4$	$3C_2$	i	$6S_4$	$8S_6$	$3\sigma_h$	$6\sigma_d$	Irreducible components
Γ_π	6	0	0	2	2	0	0	0	4	2	$a_{1g} + e_g + t_{1u}$

The metal-orbital sets of a_{1g}, e_g and t_{1u} symmetry participate in σ-bonding by interacting with the same symmetry SALCs sets to produce σ-bonding and antibonding molecular orbitals. However, the triply degenerate t_{2g} orbitals set on the metal remains nonbonding as there no ligand orbitals of this symmetry. The exact nature of the "symmetry adapted linear combination of atomic orbitals" or simply SALCs is quite complex and is beyond the scope of this volume but still we can simply give a superficial explanation for these ligand orbitals. The pictorial representation of various SALC orbitals in octahedral complexes, capable of σ-overlap with metal orbitals, can be given as:

1. If the six atomic orbitals of six ligands are pointing their positive lobes towards metal's *s*-orbital, then the composite orbital becomes:

$$\varphi_1 = \sigma_1 + \sigma_2 + \sigma_3 + \sigma_4 + \sigma_5 + \sigma_6 \qquad (1)$$

The pictorial representation is given below.

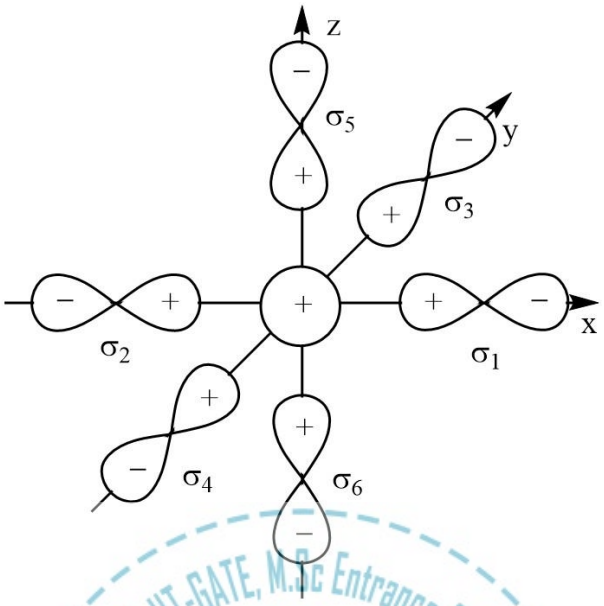

Figure 4. The combination of ligand orbitals overlapping with *s*-orbital of the metal center.

2. The p_x-orbital of metal center can overlap with ligands atomic orbital approaching along the *x*-axis. Hence, the composite orbital becomes:

$$\varphi_2 = \sigma_1 - \sigma_2 \qquad (2)$$

The pictorial representation is given below.

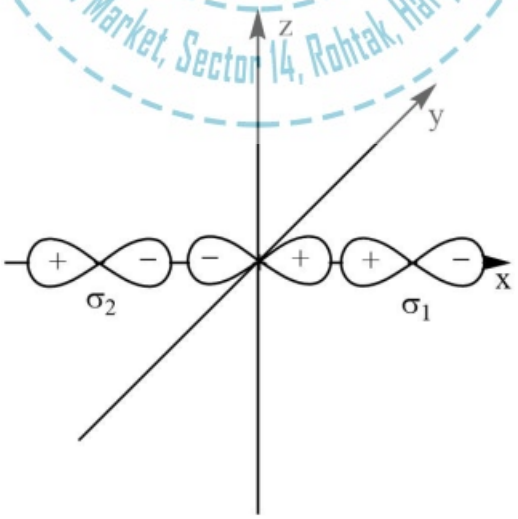

Figure 5. The combination of ligand orbitals overlapping with p_x-orbital of the metal center.

3. The p_y-orbital of metal center can overlap with ligands atomic orbital approaching along y-axis. Hence, the composite orbital becomes:

$$\varphi_3 = \sigma_3 - \sigma_4 \tag{3}$$

The pictorial representation is given below.

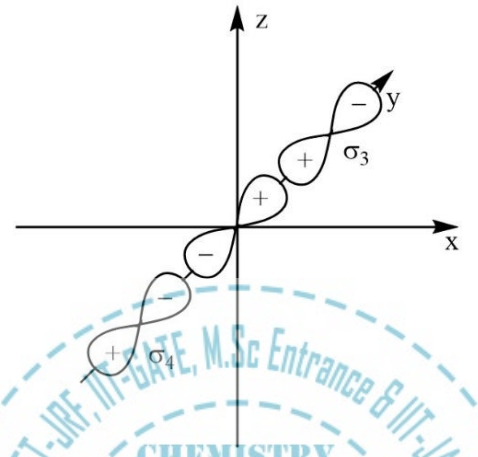

Figure 6. The combination of ligand orbitals overlapping with p_y-orbital of the metal center.

4. The p_z-orbital of metal center can overlap with ligands atomic orbital approaching along z-axis. Hence, the composite orbital becomes:

$$\varphi_4 = \sigma_5 - \sigma_6 \tag{4}$$

The pictorial representation is given below.

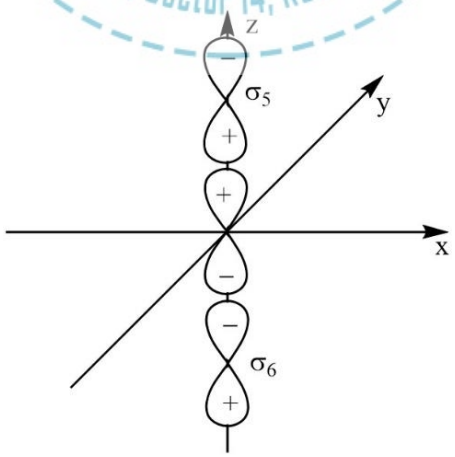

Figure 7. The combination of ligand orbitals overlapping with p_z-orbital of the metal center.

5. The $d_{x^2-y^2}$ orbital of metal center can overlap with ligands atomic orbital approaching along x and y-axis. Hence, the composite orbital becomes:

$$\varphi_5 = \sigma_1 + \sigma_2 - \sigma_3 - \sigma_4 \tag{5}$$

The pictorial representation is given below.

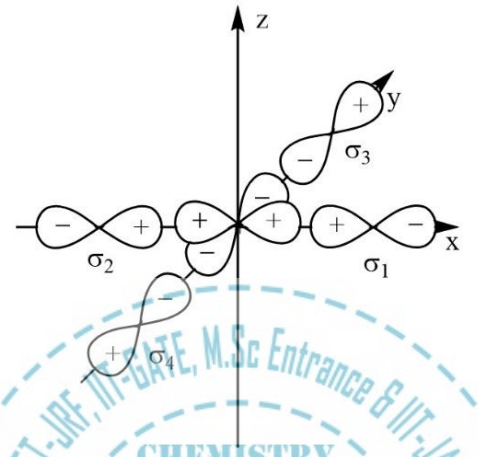

Figure 8. The combination of ligand orbitals overlapping with $d_{x^2-y^2}$ orbital of the metal center.

6. The d_{z^2} orbital of metal center can overlap with ligands atomic orbital approaching along x, y and z-axis. Hence, the composite orbital becomes:

$$\varphi_6 = \sigma_5 + \sigma_6 - \sigma_1 - \sigma_2 - \sigma_3 - \sigma_4 \tag{6}$$

The pictorial representation is given below.

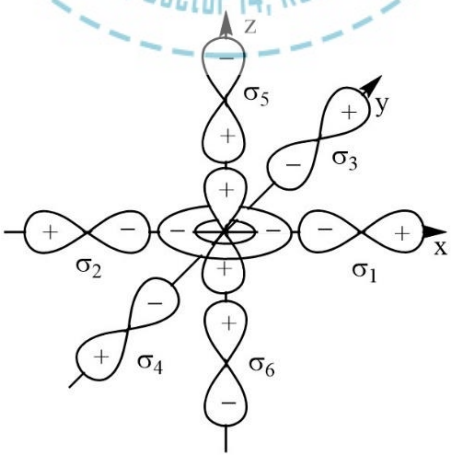

Figure 9. The combination of ligand orbitals overlapping with d_{z^2} orbital of the metal center.

The overall molecular orbital energy level diagram for σ-bonding in octahedral complexes can be shown as:

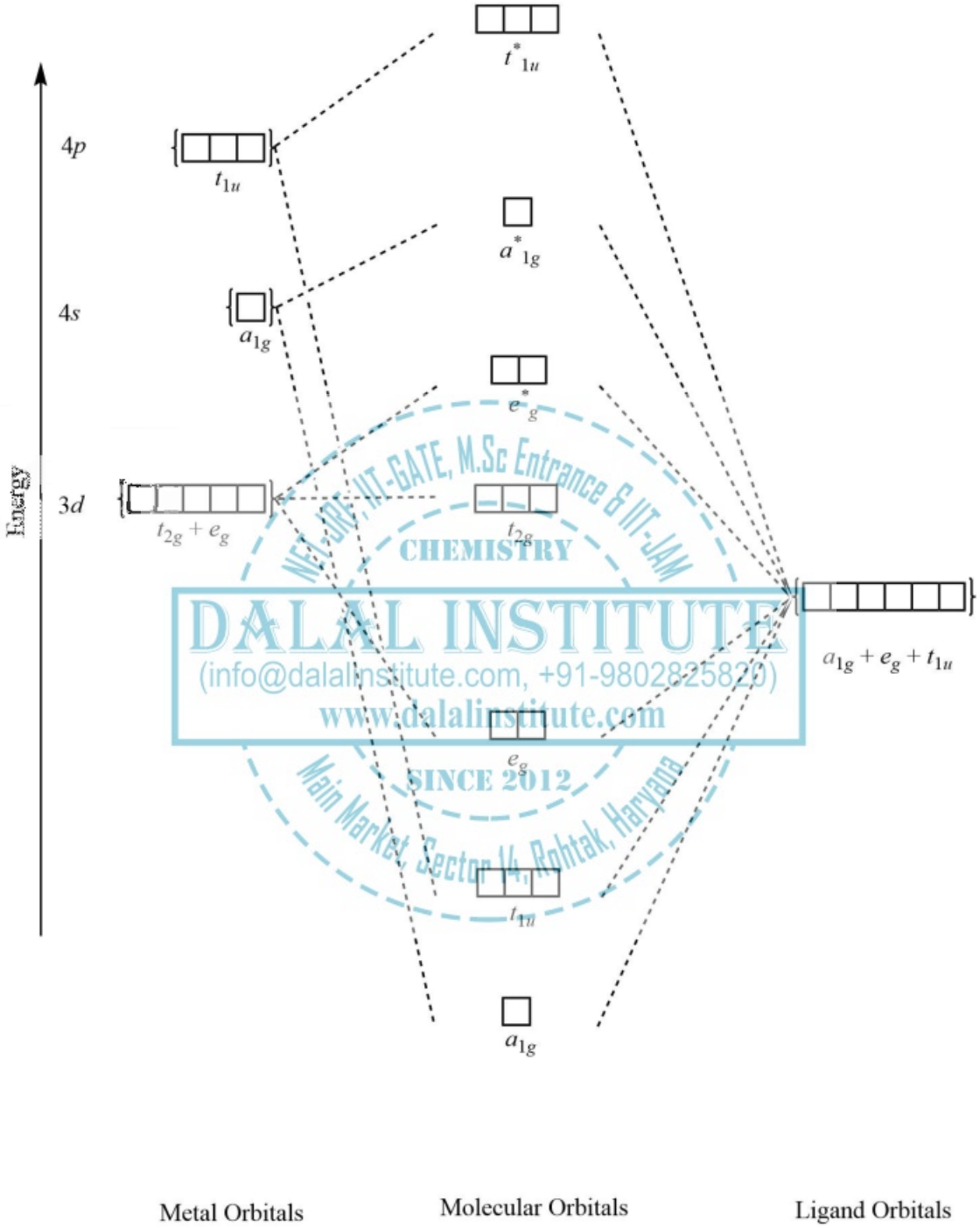

Figure 10. The formation of σ-molecular orbitals (bonding, antibonding and non-bonding) in octahedral complexes of transition metals.

The φ_1 composite orbital of a_{1g} symmetry interacts with a_{1g} orbital set of metal ions and produces one bonding (a_{1g}) and one antibonding molecular orbital (a^*_{1g}). The φ_2, φ_3 and φ_4 composite orbital set of t_{1u} symmetry interacts with t_{1u} orbital set of metal ions and produces triply-degenerate bonding (t_{1u}) and triply-degenerate antibonding molecular orbital (t^*_{1u}) set. The φ_5 and φ_6 composite orbital set of e_g symmetry interacts with e_g orbital set of metal ions and produces doubly-degenerate bonding (e_g) and doubly-degenerate antibonding molecular orbital (e^*_g) set. The t_{2g} orbital set of the metal center remains non-bonding in nature. The electron-filling in various orbitals is done in accordance with the Aufbau principle, Hund's rule and Pauli exclusion principle.

Some typical explanations in the view of MO-theory are:

i) Spin only magnetic moments: Just like crystal field theory, MO-theory can also be used to rationalize the spin only magnetic moments of different transition metal complexes. For instance, 5.9 B.M. magnetic moment of $[Mn(H_2O)_6]^{2+}$ is generated when seventeen electrons (five from Mn^{2+} and twelve electrons from six aquo ligands) are filled in different molecular orbitals. Twelve out of seventeen electrons occupy six bonding molecular orbitals of a_{1g}, t_{1u} and e_g. Three out of the remaining five electrons are filled in nonbonding t_{2g} and the last two electrons occupy e^*_g giving a total of five unpaired electrons.

ii) 18- electron rule: It is a well-known fact that metal carbonyls and many other complexes follow 18-electron rule quite well. This is also analyzed in terms of effective atomic number which suggests that a total of 18-electrons in the valence shell generally makes overall electron-count to resemble a noble gas core. However, a strong basis for this rule can found in molecular orbital theory. Six bonding molecular orbitals can accommodate a total of 12 electrons and only six electrons can be filled in the non-bonding t_{2g}. Any extra electron is bound to occupy the antibonding e^*_g orbital and hence affects the stability.

iii) The splitting of *d*-orbital: According to crystal field theory, the splitting, Δ_o of *d*-orbital in t_{2g} and e_g is produced by the difference in the Coulombic repulsion experienced various metal orbitals. However, the molecular orbital theory sees the splitting of *d*-orbital as a result of the interaction of metal orbitals with ligand orbitals and labels it as splitting between nonbonding t_{2g} and antibonding e^*_g.

iv) High spin – low spin complexes: Just like in the case of crystal field theory, the magnitude of Δ_o decides the multiplicity nature of the complexes. If the separation between nonbonding t_{2g} and antibonding e^*_g is pretty large, the electrons prefer to pair up with the electrons already present in nonbonding t_{2g} and the complex becomes low-spin. On the other side, If the separation between nonbonding t_{2g} and antibonding e^*_g is small, the electrons prefer to occupy antibonding e^*_g and the complex becomes high-spin. For example, in $[Co(NH_3)_6]^{3+}$, the magnitude of Δ_o is very large and the configuration becomes t_{2g}^6, e^{*0}_g. Furthermore, the comparatively lower stability and weaker metal-ligand bond in high spin complexes may be attributed to the presence of electrons in a molecular orbital of antibonding nature.

v) Jahn-Teller distortions: The concept of molecular orbital theory can also be used to rationalize the *z*-out or *z*-in distortion of the octahedral metal complexes. For example, octahedral complexes of Cu^{2+} ion have been known to undergo Jahn-Teller distortion due to d^9 configuration. According to molecular orbital theory, the electronic configuration octahedral complexes of Cu^{2+} will be t_{2g}^6, e^{*3}_g. Now, as the energy of e_g^* molecular

orbital is close to the pure atomic orbitals of metal ion, e_g^* would resemble more to the metal orbitals than the ligand's. Therefore, we can approximate e_g^* to pure $d_{x^2-y^2}$ and d_{z^2}. Now if the configuration is $(d_{x^2-y^2})^1 (d_{z^2})^2$, higher antibonding electron density along z-axis would result in a weaker bond and an elongation of bonds would take place along z-axis, giving a z-out distortion. On the other hand, if the configuration is $(d_{x^2-y^2})^2 (d_{z^2})^1$, higher antibonding electron density along x *and* y-axis would result in a weaker bond and an elongation would take place along x and y-axis, giving a z-in distortion.

vi) Variation of ionic radii: Experimental values of ionic radii of central metal ions in bivalent salts of first transition series were very well explained by the crystal field theory. The same can be done in the frame of molecular orbital theory. The decrease in ionic radii, when one moves from Ca^{2+} to V^{2+}, may be attributed to the increasing magnitude of effective nuclear charge while the filling of valence electrons takes place in nonbonding t_{2g}. However, after V^{2+}, the fourth electron in Cr^{2+} is filled in antibonding e^* and this effect makes the metal-ligand bond to increase, which in turn results in an increment in effective ionic radius. This trend continues up to Mn^{2+}, but as we move from Fe^{2+} to Ni^{2+}, the electron filling again goes to nonbonding t_{2g} and thus thereby decreases the ionic radii. The ninth and tenth electron in Cu^{2+} and Zn^{2+} are filled in antibonding e^* and therefore, the effective ionic radius increases again. The whole situation creates two minima in effective ionic radii, one for V^{2+} and other for Ni^{2+}.

It is worth to note down that the more sophisticated rationalization of the MO-diagram for octahedral complexes can be given in the terms of molecular symmetry combined with detailed quantum mechanics involved. In general practice, six symmetry-adapted linear combinations (SALCs) of atomic orbitals, corresponding to the irreducible components of the bond-vector based reducible representation, are created. The irreducible representations that these SALCs span to are a_{1g}, t_{1u} and e_g. The metal also has six valence orbitals that span the same irreducible representations (s-orbital is labeled as a_{1g}, a set of three p-orbitals is labeled t_{1u}, and the d_{z^2} and $d_{x^2-y^2}$ orbitals are labeled e_g). The six σ-bonding molecular orbitals result from the combinations of ligand SALC's with metal orbitals of the same symmetry.

➢ *Tetrahedral Complexes*

In tetrahedral complexes, the molecular orbitals created by the coordination profile can be seen as resulting from the donation of one electron pair by each of four σ-donor ligands to the d-orbitals on the transition metal. The visualization of the composite orbital of a tetrahedral complex in the molecular orbital framework is quite difficult because of the absence of the centre of symmetry. However, the symmetry designations of different metal orbitals taking part in this type of overlap can still be given as:

s	–	a_1
p_x, p_y, p_z	–	t_2
d_{xy}, d_{xz}, d_{yz}	–	t_2
$d_{z^2}, d_{x^2-y^2}$	–	e

The symmetry adapted linear combinations of atomic orbitals (SALCs) for metal-ligand direct overlap can be obtained just by resolving the reducible representation based on the bond vectors along the axis of σ-overlap. As there is a total of four bond vectors for the metal-ligand σ-bonding, the four-dimensional reducible representation will be obtained.

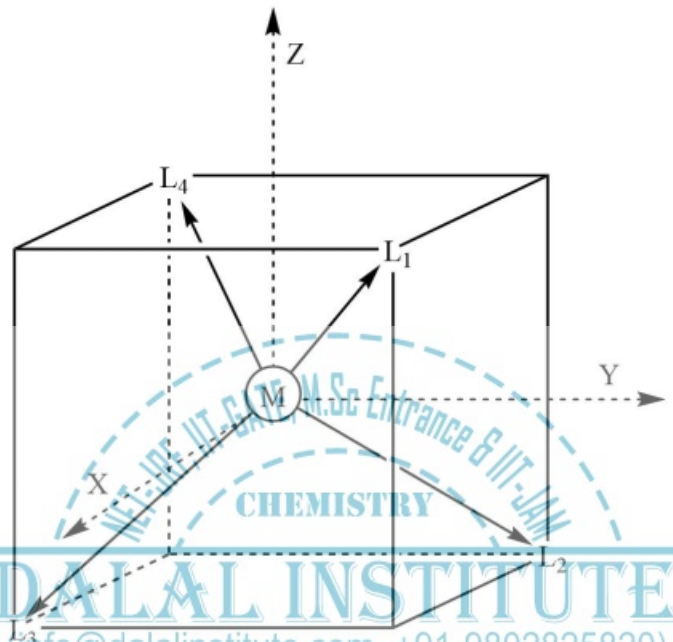

Figure 11. The σ-basis set for ligand orbitals in tetrahedral complexes.

The symmetry adapted linear combinations of these fall into two (one singly and one triply degenerate) irreducible representations labeled as a_1 and t_2. The symmetry designations of different ligand orbitals taking part in tetrahedral overlap are:

Table 2. Reducible representation based on perpendicular vectors in a tetrahedral geometry.

T_d	E	$8C_3$	$3C_2$	$6S_4$	$6\sigma_d$	Irreducible components
Γ_π	4	1	0	0	2	$a_1 + t_2$

The d_{xy}, d_{xz} and d_{yz} orbitals set on the metal also have t_2-symmetry. Similarly, the p_x, p_y and p_z-orbital set of the metal also has t_2 symmetry which resembles with the symmetry of one of SALCs set on ligands. Therefore, these same-symmetry (t_2) sets from metal and ligand interact to create three bonding and antibonding molecular orbitals. Moreover, *s*-orbital on metal has a_1-symmetry and hence mix-up with one of ligand SALC with a_1-symmetry. This also results in one bonding and one antibonding molecular orbital. One metal-orbital set of a_1 symmetry and two sets of t_2 symmetry participate in σ-bonding while the doubly

degenerate *e*-symmetry set remains nonbonding. The overall molecular orbital energy level diagram for σ-bonding in tetrahedral complexes can be shown as:

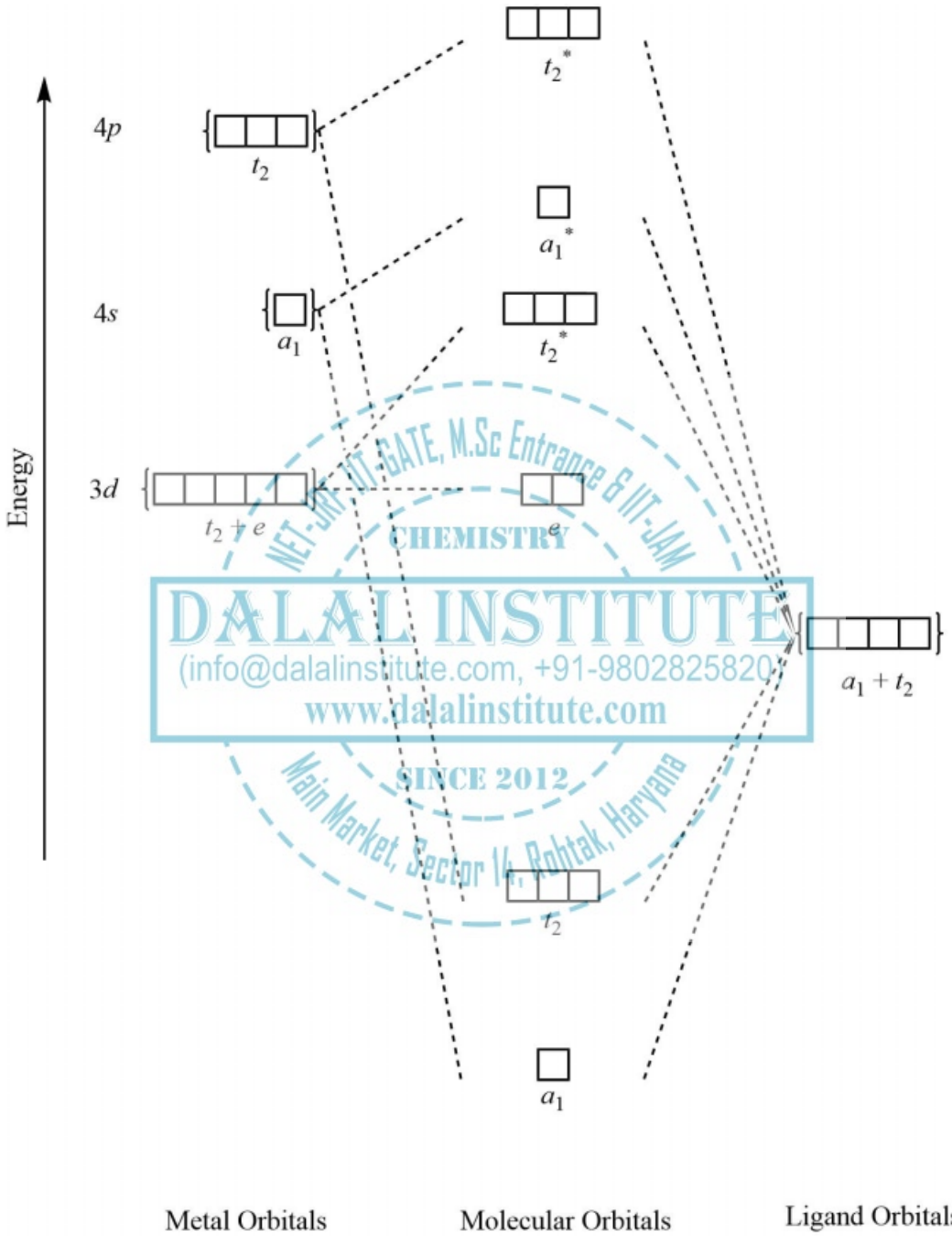

Figure 12. The formation of σ-molecular orbitals (bonding, antibonding and non-bonding) in tetrahedral complexes of transition metals.

➢ ***Square Planar Complexes***

In square-planar complexes, the molecular orbitals created by coordination can be seen as resulting from the donation of two electrons by each of four σ-donor ligands to the *d*-orbitals on the metal. The metal orbitals taking part in this type of bonding are *nd*, (*n*+1)*p* and (*n*+1)*s*. It should be noted down that not all *nd* or (*n*+1)*p* orbitals but only d_{z^2}, $d_{x^2-y^2}$, p_x and p_y-orbitals are capable of participating in the σ-overlap. The d_{xy}, d_{xz}, d_{yz} and p_z-orbitals remain non-bonding orbitals. The symmetry designations of different metal orbitals taking part in square-planar overlap are:

s	–	a_{1g}
p_x, p_y	–	e_u
d_{z^2}	–	a_{1g}
$d_{x^2-y^2}$	–	b_{1g}
p_z	–	a_{2u}
d_{xy}	–	b_{2g}
d_{yz}, d_{xz}	–	e_g

The symmetry adapted linear combinations of ligand atomic orbitals (SALCs) for metal-ligand sidewise overlap in square planar complexes can be obtained just by resolving the reducible representation based on the bond vectors along to the axis of σ-overlap. As there are total four bond vectors for the metal-ligand σ-bonding, the four-dimensional reducible representation will be obtained.

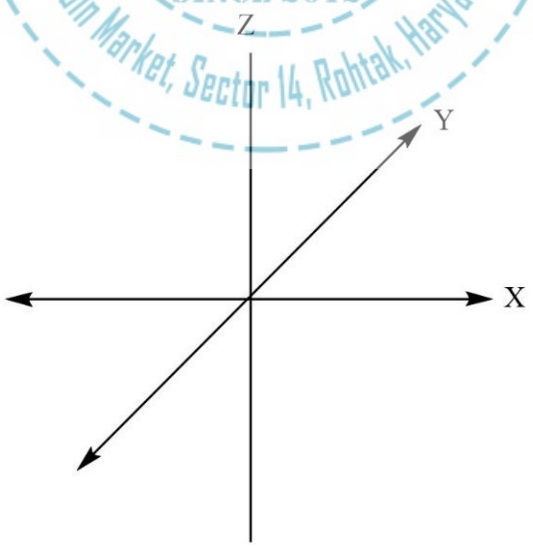

Figure 13. Continued on the next page…

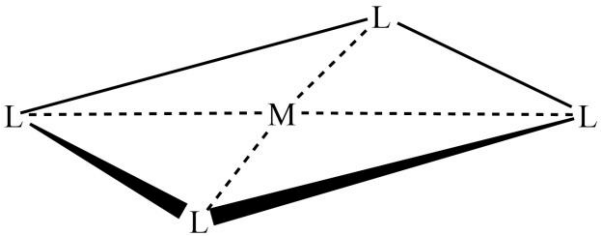

Figure 13. The σ-basis set for ligand orbitals and corresponding coordination in square-planar complexes of transition metals.

The symmetry adapted linear combinations of these fall into three irreducible representations labeled as a_{1g}, b_{1g} and e_u. The symmetry designations of different ligand SALC-orbitals taking part in square-planar overlap are:

Table 3. Reducible representation based on perpendicular vectors in square planar geometry.

D_{4h}	E	$2C_4$	C_2	$2C_2'$	$2C_2''$	i	$2S_4$	σ_h	$2\sigma_v$	$2\sigma_d$	Irreducible components
Γ_π	4	0	0	2	0	0	0	4	2	0	$a_{1g} + b_{1g} + e_u$

The irreducible components that these SALCs span to are a_{1g}, b_{1g} and e_u. The molecular orbitals of σ-bonding in square-planar complexes result from the mixing of ligand SALCs with metal orbitals of the same symmetry. Two metal-orbital sets of a_{1g} symmetry, one set of b_{1g} symmetry and one set on e_u symmetry participate in σ-bonding while the doubly degenerate e_g and singly degenerate b_{2g} sets remain nonbonding. This is quite logical because there are no ligand orbitals with these symmetry properties and hence no orbital overlap is possible. The ligands approach the metal center along the x and y-axes in such a way that their σ-symmetry orbitals form bonding and anti-bonding combinations with metal's s, p_x, p_y, d_z^2 and $d_{x^2-y^2}$ orbitals. Two a_{1g}-symmetry sets of metal orbitals (s and d_z^2) interact with the ligands SALC of the same symmetry and form three molecular orbitals. The b_{1g}-symmetry set of metal orbital ($d_{x^2-y^2}$) interact with the ligands SALC of same symmetry and form two molecular orbitals, one bonding and one of antibonding nature.

Similarly, e_u-symmetry set of metal orbitals (p_x, p_y) interacts with the ligands SALC of the same symmetry and form bonding and antibonding molecular orbital sets. A total of nine sets of molecular orbitals are formed in which electron filling has to occur. Furthermore, it should also be noted that bonding molecular orbitals are predominantly associated with ligands which can be attributed to the lower energy of ligand SALCs while the antibonding molecular orbitals are primarily associated with the metal center owing to the higher energy of its atomic orbitals. In other words, the simplistic approach can treat bonding molecular orbitals as ligand orbitals and antibonding molecular orbitals as metal orbitals.

The molecular orbital energy level diagram for σ-bonding in square-planar complexes can be shown as:

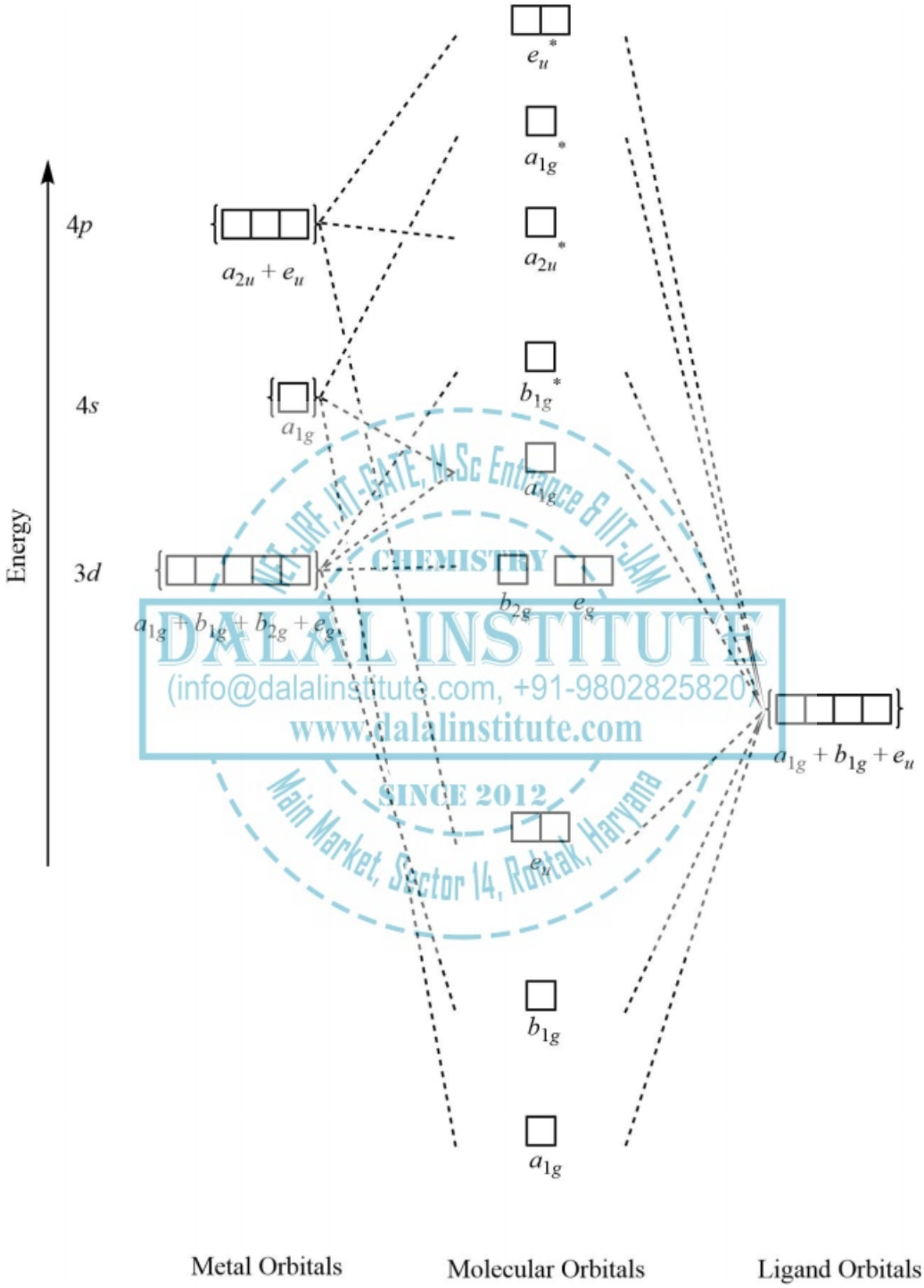

Figure 14. The generation of σ-molecular orbitals in square-planar complexes.

❖ π-Bonding and Molecular Orbital Theory

We have already studied the metal-ligand σ-overlap in the framework of molecular orbitals theory. Furthermore, this theory is also very useful for providing a rational explanation for the π-bonding in different metal-complex geometries. The basic approach remains the same except the fact that the orbital overlap in this situation is not along the internuclear axis but is sidewise in nature. The symmetry criteria governing these overlaps are absolutely clear but the extant up to which the overlap for different ligands takes place is still a matter of debate. In other words, the matching of metal and ligands orbital symmetry is not sufficient to assure the formation of π-bond as there are also some other factors (like size and energy) that signify the extent of overlap. It is quite possible that two orbital sets with the same symmetry may not be able to form molecular orbital due to a large difference in their energies.

There are four different types of metal-ligand interaction which can be resulted from the sidewise overlap of the orbitals.

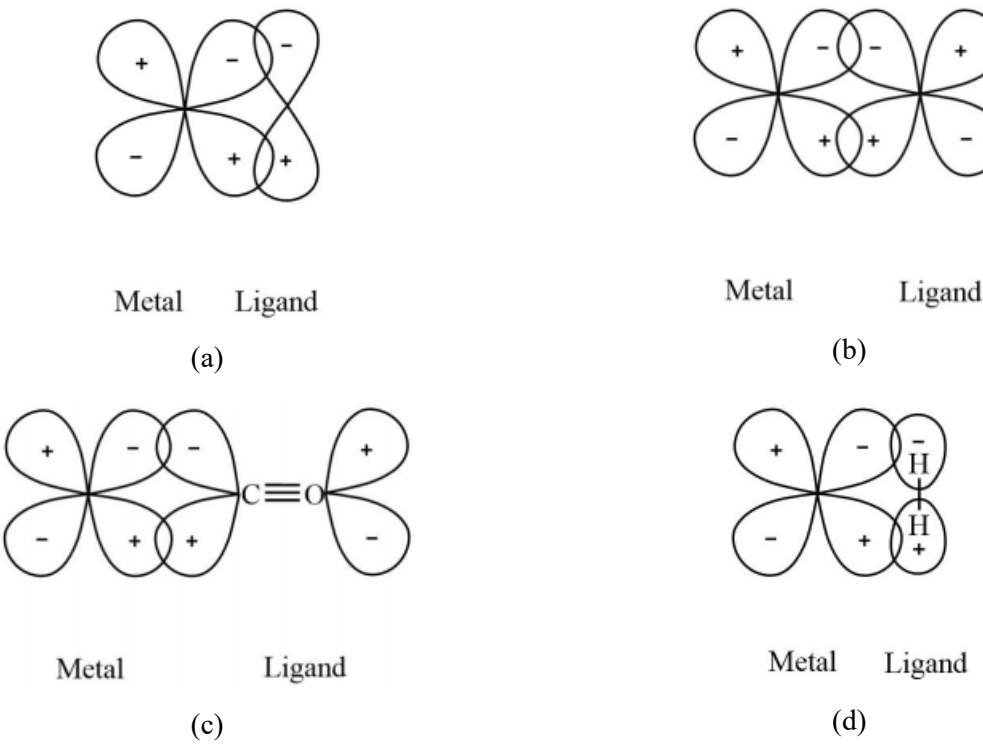

Figure 15. The sidewise overlap (π-bonding) of the *d*-orbital metal with different types of ligands orbital (a) d_π-p_π, (b) d_π-d_π, (c) d_π-π^*, (d) d_π-σ^*.

Electron density can be transferred from filled ligand orbital to the empty d-orbital of the metal center, or from the filled d-orbital of the metal to the empty orbital of the ligand.

Table 4. Different types of π-bonding and the compatibility of various ligands.

Type	Explanation	Examples of the ligands involved
d_π-p_π	Transfer of electron density from filled *p*-orbital of the ligand to the empty *d*-orbital of the metal.	RS^-, RO^-, O^{2-}, F^-, Cl^-, Br^-, I^-, R_2N^-
d_π-d_π	Transfer of electron density from filled *d*-orbital of the metal to the empty *d*-orbital of the ligand.	R_2S, R_3P, R_3As
d_π-π^*	Transfer of electron density from filled *d*-orbital of the metal to the empty π^*-orbital of the ligand.	CN^-, CO, RNC, N_2, NO_2, ethylene, pyridine
d_π-σ^*	Transfer of electron density from filled *d*-orbital of the metal to the empty σ^*-orbital of the ligand.	R_3P, H_2, alkanes

It can be seen from the above table that some ligands belong to more than one category and hence can use more than one type orbitals for π-bonding. However, it is observed that the contribution from one type of orbitals dominates the other in many cases. For instance, R_3P can accept *d*-electron density from metal in its empty *d*-orbital, or in the antibonding σ^* which is also greater in magnitude. Similarly, I^- also has the ability to donate electron from its filled *p*-orbital, or to accept electron density in its low lying empty *d*-orbitals.

The generally accepted explanation for the π-bonding in transition metal complexes of different geometry can be given as:

- ***π-Bonding in Octahedral Complexes***

The π-bonding in octahedral complexes can happen in two ways; one through ligand *p*-orbitals that are not being used in σ bonding and other via π or π^* molecular orbitals present on the ligand. The symmetry designations of different metal orbitals taking part in octahedral overlap are:

d_z^2, $d_{x^2-y^2}$ – e_g

s – a_{1g}

p_x, p_y, p_z – t_{1u}

d_{xy}, d_{xz}, d_{yz} – t_{2g}

The symmetry adapted linear combinations of atomic orbitals (SALCs) for metal-ligand sidewise overlap can be obtained just by resolving the reducible representation based on the displacement vectors

perpendicular to the axis of σ overlap. As each of the six ligands has two basis-vectors for π-symmetry, there are twelve in total.

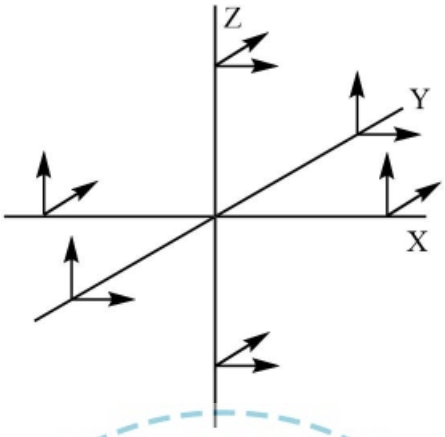

Figure 16. The π-basis set for ligand orbitals in octahedral complexes.

The symmetry adapted linear combinations of these fall into four triply degenerate irreducible representations labeled as t_{1g}, t_{2g}, t_{1u} and t_{2u}. The symmetry designations of different metal orbitals taking part in octahedral overlap are:

Table 5. Reducible representation based on perpendicular vectors in the octahedral geometry.

O_h	E	$8C_3$	$6C_2$	$6C_4$	$3C_2$	i	$6S_4$	$8S_6$	$3\sigma_h$	$6\sigma_d$	Irreducible components
Γ_π	12	0	0	0	–4	0	0	0	0	0	$t_{1g} + t_{2g} + t_{1u} + t_{2u}$

Two of these aforementioned sets are of t_{2g} and t_{1u} symmetry. The d_{xy}, d_{xz} and d_{yz} orbitals set on the metal also have t_{2g} symmetry, and therefore the π-bonds formed between a central metal and six ligands also have it as these π-bonds are just formed by the overlap of two sets of orbitals with t_{2g} symmetry. Similarly, the p_x, p_y and p_z-orbital set of the metal has t_{1u} symmetry which resembles with the symmetry of ligands SALCs. Therefore, these same-symmetry (t_{1u}) sets from metal and ligand may also interact to create bonding and antibonding molecular orbitals. However, the participation of t_{1u} set of the metal in π-overlap is highly disliked because the orbitals corresponding to this set are already being used in stronger σ-bonding and any deviation from this state is bound to destabilize the complex.

Hence, the SALC sets of t_{1g}, t_{2u} and also t_{1u} remain nonbonding. The pictorial representation of different SALC-orbitals in octahedral complexes, capable of π-overlap with metal orbitals, can be given as:

1. If four perpendicular *p*-orbitals of four ligands approaching along *x* and *y*-axis are pointing their lobes towards metal's d_{xy}-orbital in a sidewise manner, then the composite orbital becomes:

$$\varphi_1 = \pi_1 - \pi_2 + \pi_3 - \pi_4 \quad (7)$$

The pictorial representation is given below.

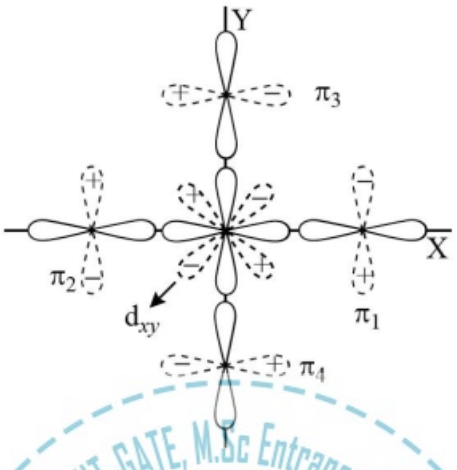

Figure 17. The combination of ligand orbitals overlapping with d_{xy}-orbital of the metal centre.

2. If four perpendicular *p*-orbitals of four ligands approaching along *y* and *z*-axis and are pointing their lobes towards metal's d_{yz}-orbital in a sidewise manner, then the composite orbital becomes:

$$\varphi_2 = \pi_3 - \pi_4 + \pi_5 - \pi_6 \quad (8)$$

The pictorial representation is given below.

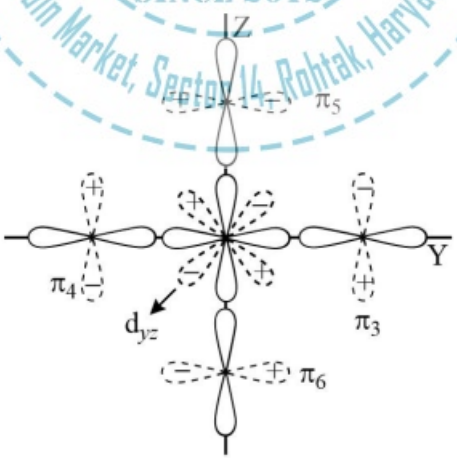

Figure 18. The combination of ligand orbitals overlapping with d_{yz}-orbital of the metal center.

3. If four perpendicular *p*-orbitals of four ligands approaching along *x* and *z*-axis are pointing their lobes towards metal's d_{xz}-orbital in a sidewise manner, then the composite orbital becomes:

$$\varphi_3 = \pi_1 - \pi_2 + \pi_5 - \pi_6 \quad (9)$$

The pictorial representation is given below.

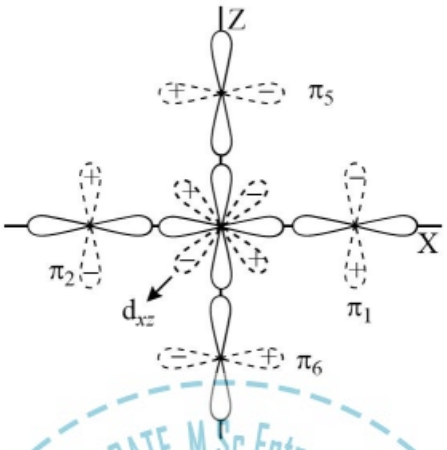

Figure 19. The combination of ligand orbitals overlapping with d_{xz}-orbital of the metal center.

Molecular orbitals and the effect of π-bonding on crystal field splitting can be categorized in three ways as follows:

1. When ligand π-orbitals are filled and are of lower energy: The one form of coordinative π-bonding is ligand-to-metal bonding. This situation arises when the t_{2g}-symmetry *p* or π-orbitals on the ligands are filled and are low in energy. They combine with the d_{xy}, d_{xz} and d_{yz} orbitals on the metal and donate electrons to the resulting π-symmetry bonding orbital between them and the metal.

The metal-ligand bond is somewhat strengthened by this interaction, but the complementary anti-bonding molecular orbital from metal-ligand overlap is not higher in energy than the antibonding molecular orbital from the σ-bonding. The molecular orbital of t_{2g}^* are greater in energy than nonbonding sets of t_{1g}, t_{2u} and t_{1u}. On the other hand, the bonding molecular orbitals of t_{2g} are lower in energy than that of nonbonding SALCs of the ligands.

Therefore, when 36 electrons (12×2 from π-bonding and 6×2 from σ-bonding) from ligands are filled in the molecular orbitals, they will completely saturate the a_{1g}-bonding, t_{1u}-bonding, e_g-bonding, t_{2g}-bonding and the nonbonding sets of t_{1g}, t_{2u} and t_{1u}. The electron previously filled in *d*-orbital of the free metal ion can now be considered as distributed between t_{2g}^* and e_g^*. Hence, the crystal field splitting Δ_o decreases when ligand to metal bonding takes place.

The overall molecular orbital energy level diagram for this type of π-bonding in octahedral complexes can be shown as:

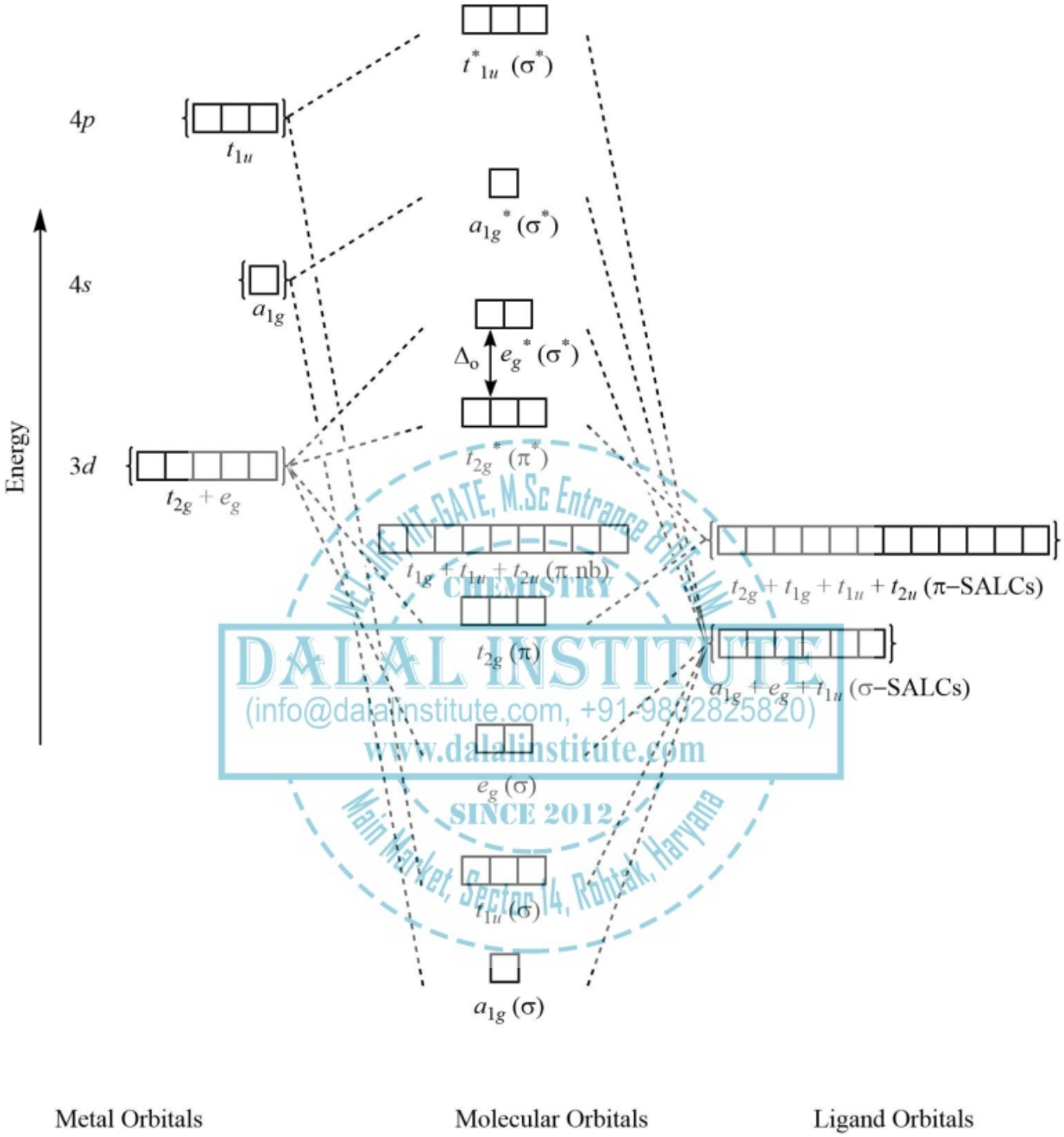

Figure 20. The generation of π and σ-molecular orbitals in octahedral complexes.

2. When ligand π-orbitals are empty and are of higher energy: The second important form of π-bonding in coordination complexes is metal-to-ligand π bonding, also called π-backbonding. It occurs when the LUMOs (lowest unoccupied molecular orbitals) of the ligand are anti-bonding π^*-orbitals and are high in energy. The ligands end up with electrons in their π^* molecular orbital, so the corresponding π-bond within the ligand

weakens. The complementary anti-bonding molecular orbital from metal-ligand overlap is higher in energy than both, the first antibonding molecular orbital from the σ-bonding (e_g^*), and the nonbonding sets of t_{1g}, t_{2u} and t_{1u}. On the other hand, the bonding molecular orbitals of t_{2g} are higher in energy than all σ bonding molecular orbitals. The overall molecular orbital energy level diagram for this type of π-bonding in octahedral complexes can be shown as:

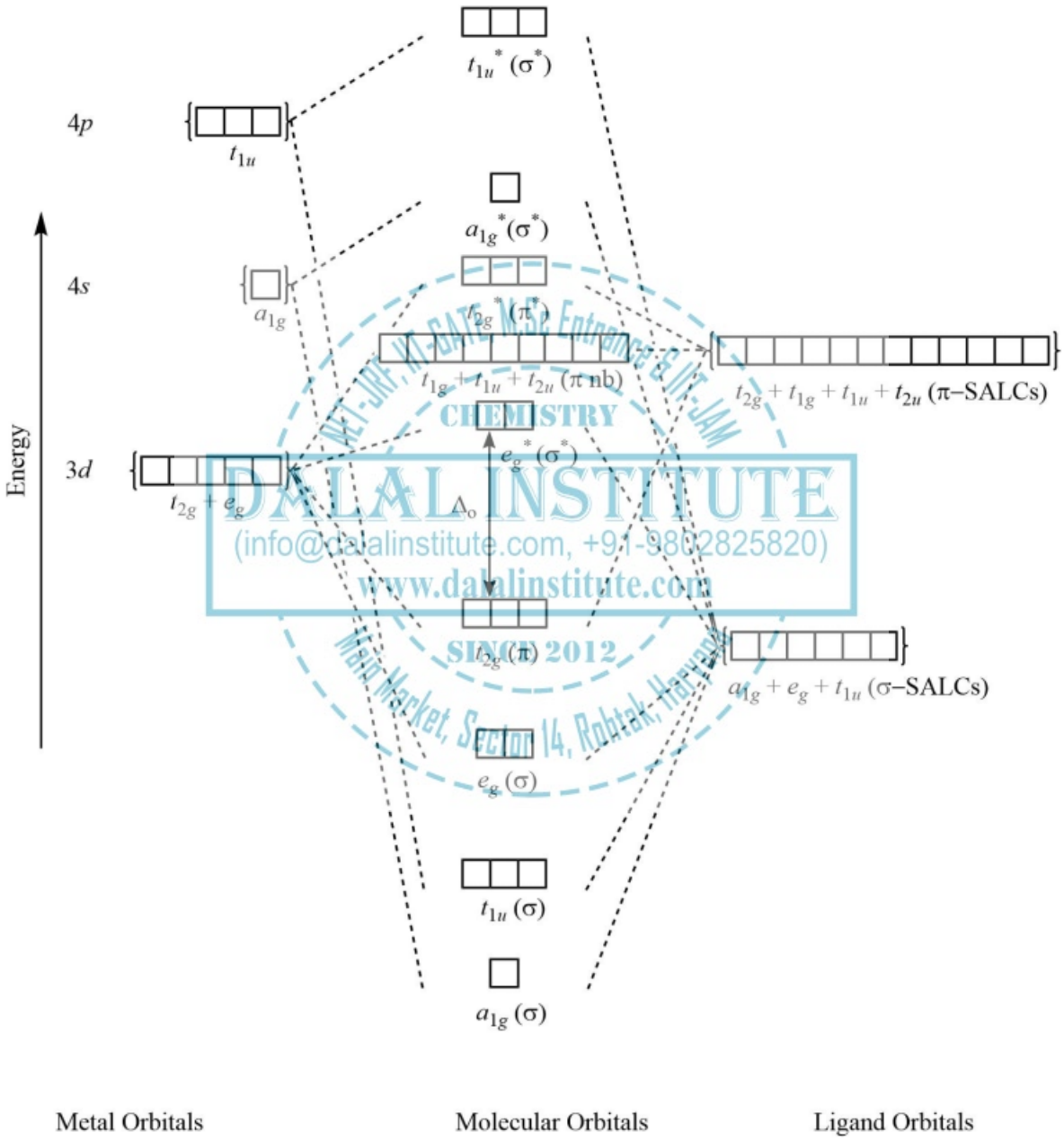

Figure 21. The generation of π and σ-molecular orbitals in octahedral complexes.

Therefore, when twelve electrons (12×0 from π-bonding and 6×2 from σ-bonding) from ligands are filled in the molecular orbitals, they will completely saturate the a_{1g}-bonding, t_{1u}-bonding and e_g-bonding. The electron previously filled in *d*-orbital of the free metal ion can now be considered as distributed between t_{2g} and e_g^*. Hence, the crystal field splitting Δ_o increases and the bond between the ligand and the metal strengthens when metal to ligand bonding takes place.

3. When ligand π-orbitals are empty as well as filled: There are many ligands, like I^-, which have both filled *p*-orbitals as well as vacant d-orbitals of π symmetry. In these cases, the prediction of crystal field splitting energy is quite difficult as the two effects counterbalance each other to different extents for different ligands. The six bonding MOs which are formed are actually filled by the electrons coming from the ligands, and electrons from the *d*-orbitals of the metal ion occupy the nonbonding and, sometimes, antibonding molecular orbitals. The energy difference between the latter two types of MOs is called Δ_o and is determined by the nature of the π-interaction between the ligand orbitals with the *d*-orbitals on the central atom. As described above, π-donor ligands lead to a small Δ_o and are called weak- or low-field ligands, whereas π-acceptor ligands lead to a large value of Δ_o and are called strong or high-field ligands. Ligands that are neither π-donor nor π-acceptor give a value of Δ_o somewhere in-between.

The magnitude of Δ_o determines the electronic structure of d^4-d^7 metal ions., The nonbonding and antibonding MOs in types of metals complexes can be filled in two ways; the first one in which maximum possible electrons are put in the nonbonding orbitals before the antibonding filling, and second one in which maximum possible unpaired electrons are put in. The first case is labeled as low-spin, while the second is labeled as high-spin complexes. A small Δ_o can be outranked by the energetic stabilization from avoiding the electron pairing, leading to the spin-free case. On the other hand, if Δ_o is large, the spin-pairing energy would become negligible in comparison and a spin-paired state arises. An empirically-obtained list of various ligands which are arranged by the magnitude of splitting Δ they produce is called as the spectrochemical series. It can be seen that the low-field ligands are all π-donors (such as I^-), the high field ligands are π-acceptors (such as CN^- and CO), and ligands such as H_2O and NH_3, which are neither, are in the middle.

$I^- < Br^- < S^{2-} < SCN^- < Cl^- < NO^{3-} < N^{3-} < F^- < OH^- < C_2O_4^{2-} < H_2O < NCS^- < CH_3CN <$ py (pyridine) $< NH_3 <$ en (ethylenediamine) < bipy (2,2'-bipyridine) < phen (1,10-phenanthroline) $< NO_2^- < PPh_3 < CN^- <$ CO

It is also worthy to note that the electrons transfer from metal *d*-orbital to the antibonding molecular orbitals of carbonyl and its analogs is actually partial in nature. The electron-transfer increases metal-carbon bond strength but weakens the carbon–oxygen bond. The increased M–CO bond strength is obvious in the increases of vibrational frequencies for the metal–carbon bond and usually lie outside the range of normal IR spectrophotometers. Moreover, the bond length of M–CO bond is also shortened. The decreased bond strength of C–O bond is obvious from the decreasing wavenumber of ν_{CO} bands. The high stabilization which results from metal-to-ligand bonding (back-bonding) is caused by the relaxation of the negative charge from the metal center. This permits the metal ion to accept the σ-donation more effectively. The combination of ligand-to-metal σ-bonding and metal-to-ligand π-bonding is a synergic effect, as each enhances the other.

➢ *π-Bonding in Tetrahedral Complexes*

The π-bonding in tetrahedral complexes can happen in two ways; one through ligand *p*-orbitals that are not being used in σ bonding and other via π or π^* molecular orbitals present on the ligand. The symmetry designations of different metal orbitals taking part in tetrahedral overlap are:

s	–	a_1
p_x, p_y, p_z	–	t_2
d_{xy}, d_{xz}, d_{yz}	–	t_2
$d_z^2, d_{x^2-y^2}$	–	e

The symmetry adapted linear combinations of atomic orbitals (SALCs) for metal-ligand sidewise overlap can be obtained just by resolving the reducible representation based on the displacement vectors perpendicular to the axis of σ overlap. As each of the four ligands has two basis-vectors for π-symmetry, there are eight in total. Each pair of perpendicular vectors (p_x and p_y) is attached about its own *z*-axis so that all the *y*-vectors are parallel to the *xy*-plane of the tetrahedral complex.

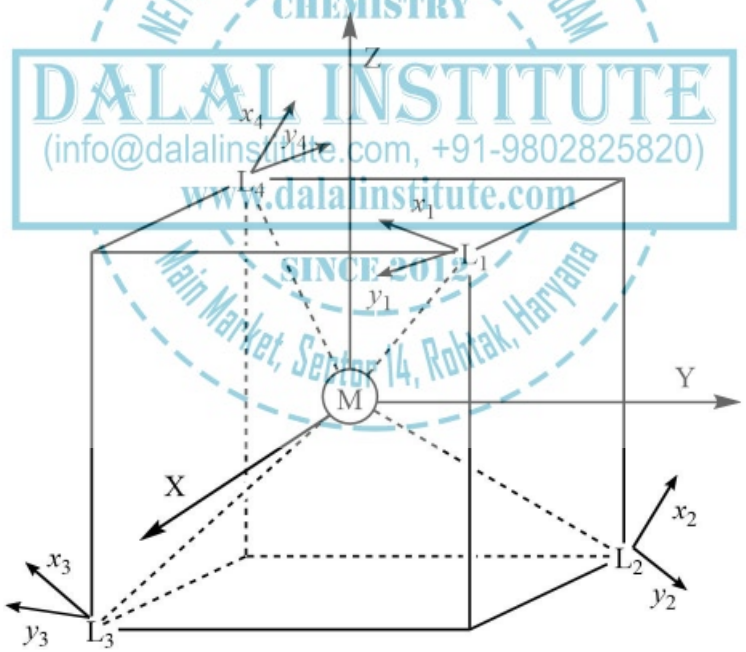

Figure 22. The π-basis set for ligand orbitals in tetrahedral complexes.

The symmetry adapted linear combinations of these fall into two doubly and on singly degenerate irreducible representations labeled as *e*, t_1 and t_2. The symmetry designations of different ligand orbitals taking part in tetrahedral overlap are:

Table 6. Reducible representation based on perpendicular vectors in the tetrahedral geometry.

T_d	E	$8C_3$	$3C_2$	$6S_4$	$6\sigma_d$	Irreducible components
Γ_π	8	–1	0	0	0	$e + t_1 + t_2$

Two of these aforementioned sets are of *e* and t_2 symmetry. The $d_{x^2-y^2}$ and d_{z^2} orbitals set on the metal also have *e*-symmetry, and therefore the π-overlap between a central metal and four ligands is possible as far as the generation of molecular orbitals with *e*-symmetry is concerned.

Similarly, the p_x, p_y and p_z-orbital set of the metal has t_2 symmetry which resembles with the symmetry of one of SALCs set on ligands. Therefore, these same-symmetry (t_2) sets from metal and ligand may also interact to create bonding and antibonding molecular orbitals. However, the π-overlap in tetrahedral complexes is not independent of the σ-bonding because the ligand SALCs and metals atomic orbital, of both types of *e* and t_2 symmetry, participate in σ as well as π-bonding.

Hence, when twenty-four electrons (8×2 from π-bonding and 4×2 from σ-bonding) from ligands are filled in the molecular orbitals, they will completely saturate the a_1 (σ), t_2 (σ), t_2 (π), *e* (π) and t_1 (π nb). The electron previously filled in *d*-orbital of the free metal ion can now be considered as distributed in e^* (π^*) and t_2^* (σ^*, π^*) which are predominantly $d_{x^2-y^2} = d_{z^2}$ and $d_{xz} = d_{yz} = d_{xy}$ in character, respectively.

Therefore, the pattern of crystal field splitting energy, provided by the molecular orbital theory, is the same as that of what it was given by crystal field theory. Moreover, the ligand to metal charge transfer spectral band can be considered as a result of the transition of an electron from nonbonding or bonding molecular orbitals to the antibonding molecular orbitals. These charge transfer peaks are very high in intensity they are spin as well as Laporte allowed in nature.

Tetrahedral complexes are almost always high-spin in nature because the energy separation between e^* (π^*) and t_2^* (σ^*, π^*) energy levels, Δ_t, is very small. That's why, during the filling of metal *d*-electrons, the promotion of electrons is always preferred over pairing. This is the same result as provided by the application of crystal field theory.

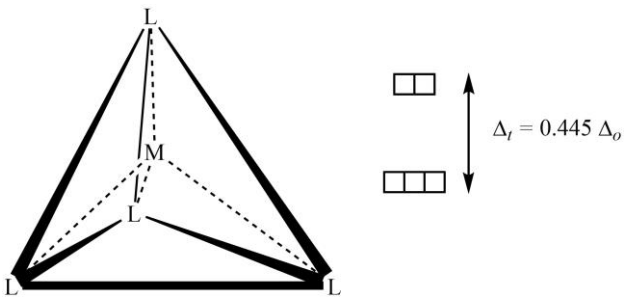

Figure 23. The crystal field splitting of *d*-subshell in tetrahedral complexes.

The overall molecular orbital energy level diagram for this type of π-bonding in tetrahedral complexes can be shown as:

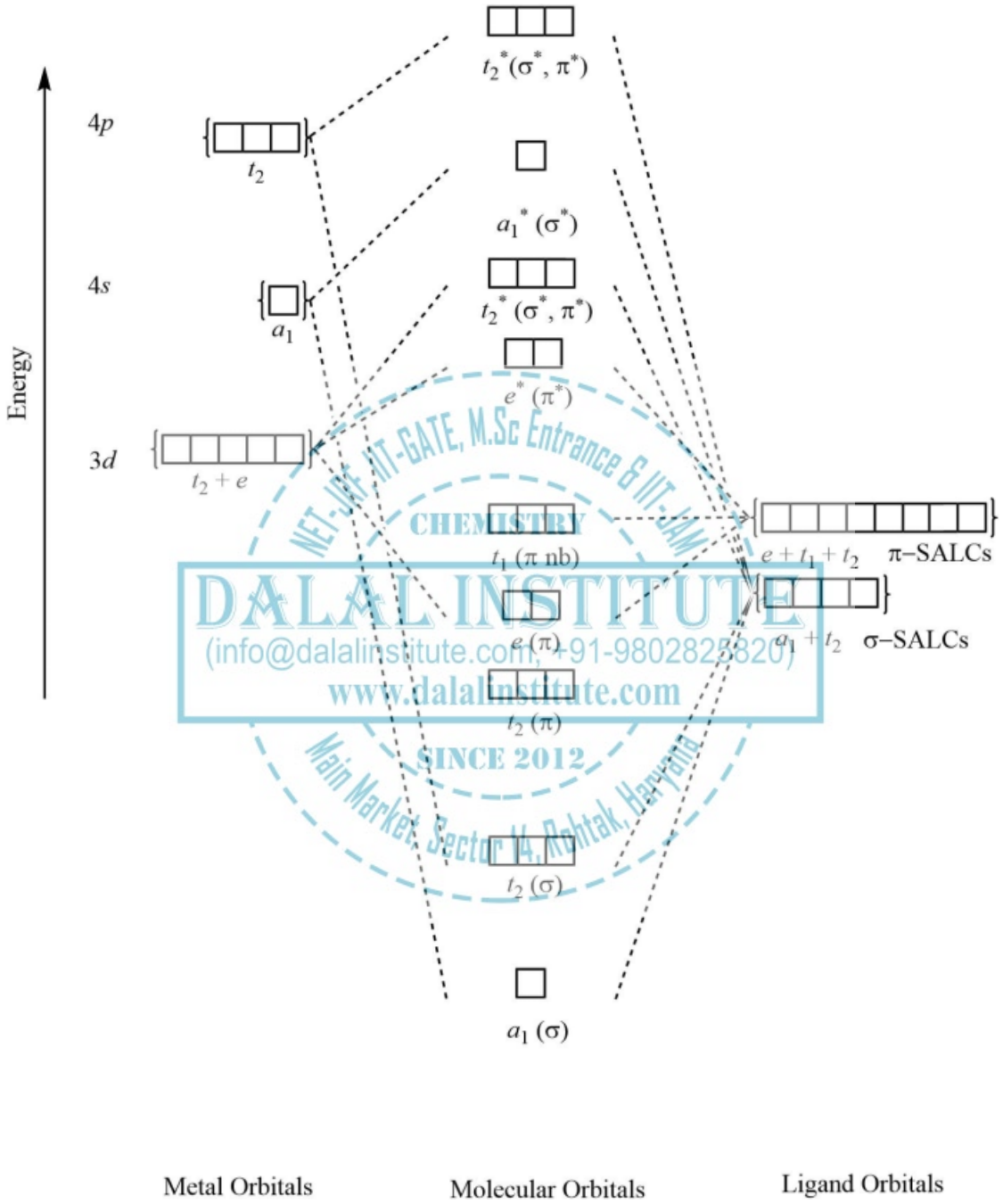

Figure 23. The generation of π and σ-molecular orbitals in four-coordinated tetrahedral complexes of transition metals.

➢ *π-Bonding in Square Planar Complexes*

The π-bonding in square planar complexes can be visualized in terms of the sidewise overlap of different kinds of orbitals on metal and ligands, having comparable energy and proper symmetry. The symmetry designations of different metal orbitals taking part in square-planar overlap are:

s	–	a_{1g}
p_x, p_y	–	e_u
d_z^2	–	a_{1g}
$d_{x^2-y^2}$	–	b_{1g}
p_z	–	a_{2u}
d_{xy}	–	b_{2g}
d_{yz}, d_{xz}	–	e_g

The symmetry adapted linear combinations of ligand atomic orbitals (SALCs) for metal-ligand sidewise overlap in square planar complexes can be obtained just by resolving the reducible representation based on the displacement vectors perpendicular to the axis of σ-overlap. As each of the four ligands has two basis-vectors for π-symmetry, there are eight in total.

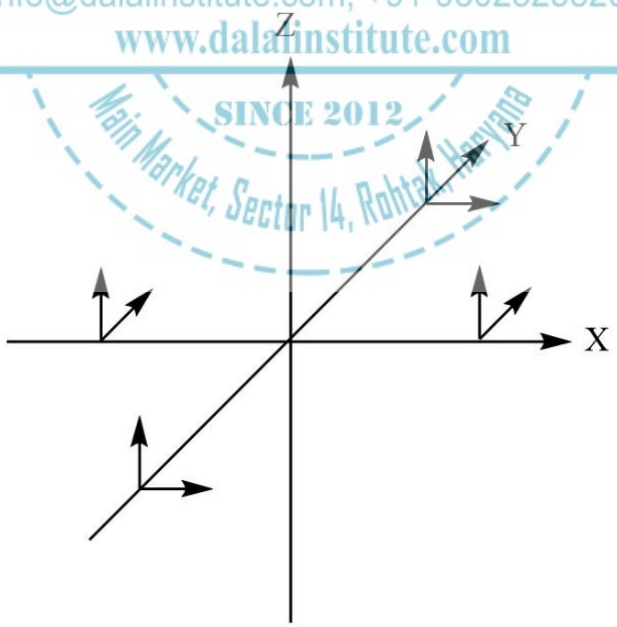

Figure 24. The complete π-basis set for ligand orbitals in square planar complexes of transition metal centers.

The symmetry adapted linear combinations of these fall into six irreducible representations labeled as a_{2g}, b_{2u}, e_u, a_{2u}, e_g and b_{2g}. The symmetry designations of different ligand SALC-orbitals taking part in square-planar overlap are:

Table 7. The complete reducible representation based on perpendicular vectors (usable in sidewise overlap) in square planar geometry.

D_{4h}	E	$2C_4$	C_2	$2C_2'$	$2C_2''$	i	$2S_4$	σ_h	$2\sigma_v$	$2\sigma_d$	Irreducible components
Γ_π	8	0	0	–4	0	0	0	0	0	0	$a_{2g} + b_{2u} + e_u + e_g + b_{2g} + a_{2u}$.

Two of these aforementioned sets, with a_{2g} and b_{2u} symmetry, remain nonbonding and are localized on the ligands. This is quite logical because there are no metal orbitals with these symmetry properties and hence no orbital overlap is possible.

The metal orbitals of e_u-symmetry take part in σ as well as π-bonding. Now, as there are two sets of SLACs with e_u-symmetry, the number of molecular orbital sets formed with e_u-symmetry is also three. The lowest energy molecular orbitals set of e_u-symmetry is primarily of σ-bonding while the higher energy molecular orbitals set is mainly π-bonding in nature. The highest doubly degenerate molecular orbitals set of e_u-symmetry is of both σ^* and π^*-antibonding character.

The d_{yz} and d_{xz} orbitals set on the metal has e_g-symmetry, which resembles with the symmetry of one of SALCs set on ligands. Therefore, these same-symmetry (e_g) sets from metal and ligand also interact to create bonding and antibonding molecular orbitals. Furthermore, the b_{2g}-symmetry d_{xy} orbital and a_{2u}-symmetry p_z orbitals on the metal interacts with b_{2g}-symmetry and a_{2u}-symmetry SALC, respectively, to produce π-bonding and antibonding molecular orbitals.

Hence, when twenty-four electrons (8×2 from π-bonding and 4×2 from σ-bonding) from ligands are filled in the molecular orbitals, they will completely saturate the $a_{1g}(\sigma)$, $b_{1g}(\sigma)$, $e_u(\sigma)$, $b_{2g}(\pi)$, $e_g(\pi)$, $a_{2u}(\pi)$, $e_u(\pi)$, $a_{2g}(\pi$ nb) and $b_{2u}(\pi$ nb). The electron previously filled in d-orbital of the free metal ion can now be considered as distributed in $e_g^*(\pi^*)$, $a_{1g}(\sigma^*)$, $b_{2g}^*(\pi^*)$ and $b_{1g}^*(\sigma^*)$ which are predominantly d_{xz}=d_{yz}, d_z^2, d_{xy} and $d_{x^2-y^2}$ in character, respectively. Hence, the pattern of crystal field splitting energy, provided by the molecular orbital theory, is the same as that of what it was given by crystal field theory. In other words, the formal electronic configuration of tetrahedral metal complexes is the same from both theories.

Moreover, the ligand to metal charge transfer spectral band can be considered as a result of the transition of an electron from nonbonding or bonding molecular orbitals to $b_{1g}^*(\sigma^*)$. These charge transfer peaks are pretty high in intensity due to their spin and Laporte allowance.

The overall molecular orbital energy level diagram for the π-bonding in square-planar complexes can be shown as:

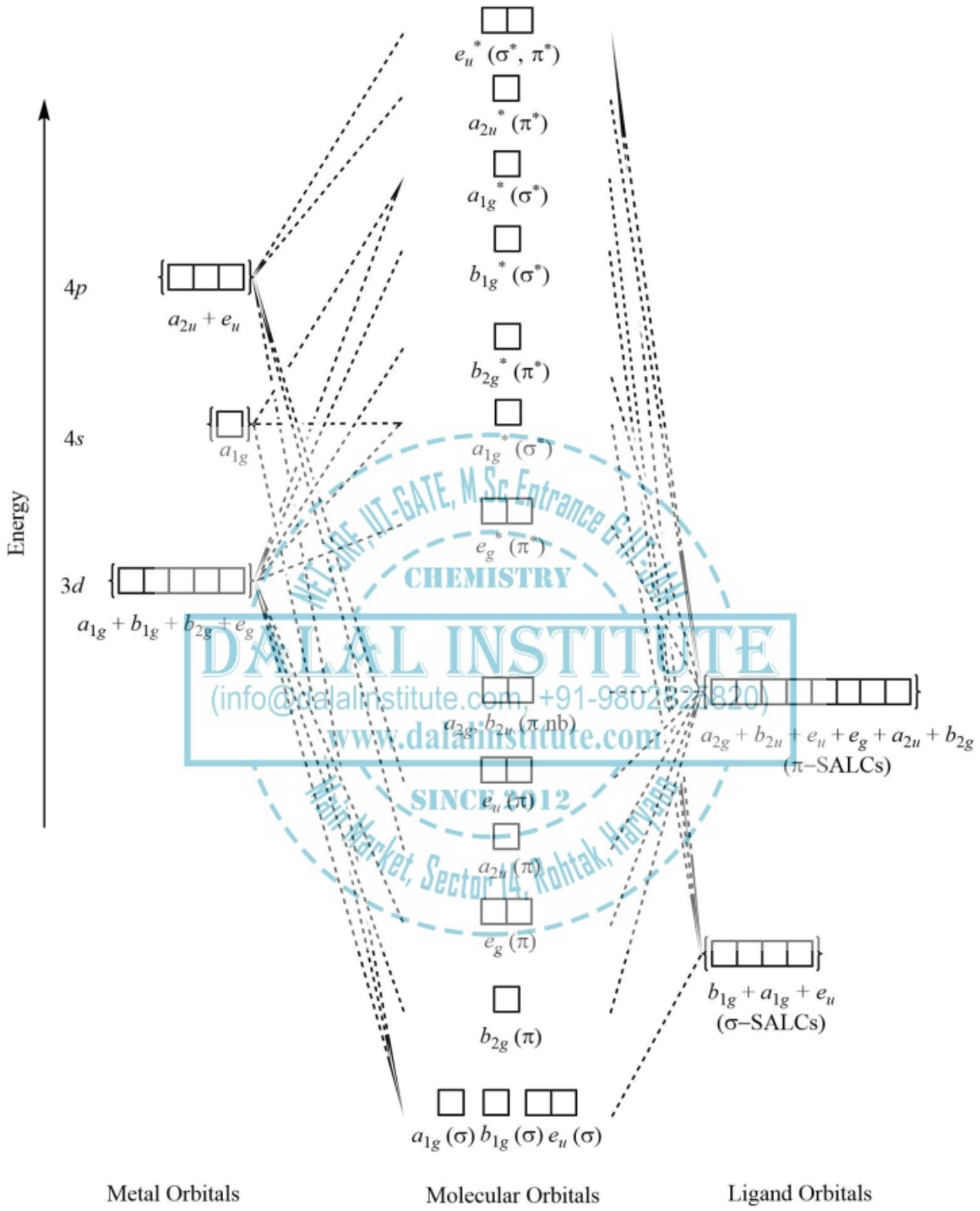

Figure 25. The generation of π and σ-molecular orbitals in square-planar complexes.

❖ Problems

Q 1. Give at least seven limitations of crystal field theory.

Q 2. Why does the crystal field theory fail to provide any rational explanation for the nephelauxetic effect?

Q 3. Discuss the "superexchange phenomenon" as an evidence for the presence of covalent-character in metal-ligand bonds.

Q 4. Write down the main postulates of molecular orbital theory for metal complexes.

Q 5. Explain the metal-ligand σ-bonding for octahedral complexes in the molecular orbital framework.

Q 6. Draw and discuss the molecular orbital energy level diagram involving σ-bonding for tetrahedral complexes.

Q 7. How does the π-bonding affect the magnitude of crystal field splitting in octahedral complexes when ligand π-orbitals are empty and are high in energy?

Q 8. Explain the metal-ligand π-bonding for octahedral complexes in the molecular orbital framework.

Q 9. Draw and discuss the molecular orbital energy level diagram involving π-bonding for tetrahedral complexes.

Q 10. Draw the molecular orbital energy level diagram for π-bonding for square-planar complexes. Also, explain ligand to metal charge transfer in brief.

❖ Bibliography

[1] B. R. Puri, L. R. Sharma, K. C. Kalia, *Principals of Inorganic Chemistry*, Milestone Publishers, Delhi, India, 2012.

[2] J. E. Huheey, E. A. Keiter, R. L. Keiter, *Inorganic Chemistry: Principals of Structure and Reactivity*, HarperCollins College Publishers, New York, USA, 1993.

[3] B. W. Pfennig, *Principles of Inorganic Chemistry*, John Wiley & Sons, New Jersey, USA, 2015.

[4] F. A. Cotton, *Chemical Applications of Group Theory*, John Wiley & Sons, New Jersey, USA, 2006.

[5] N. N. Greenwood, A. Earnshaw, *Chemistry of the Elements*, Butterworth-Heinemann, Oxford, Britain, 1998.

[6] J. E. House, *Inorganic Chemistry*, Academic Press, California, USA, 2008.

[7] D. Shriver, M. Weller, T. Overton, J. Rourke, F. Armstrong, *Inorganic Chemistry*, W. H. Freeman and Company, New York, USA, 2014.

Home

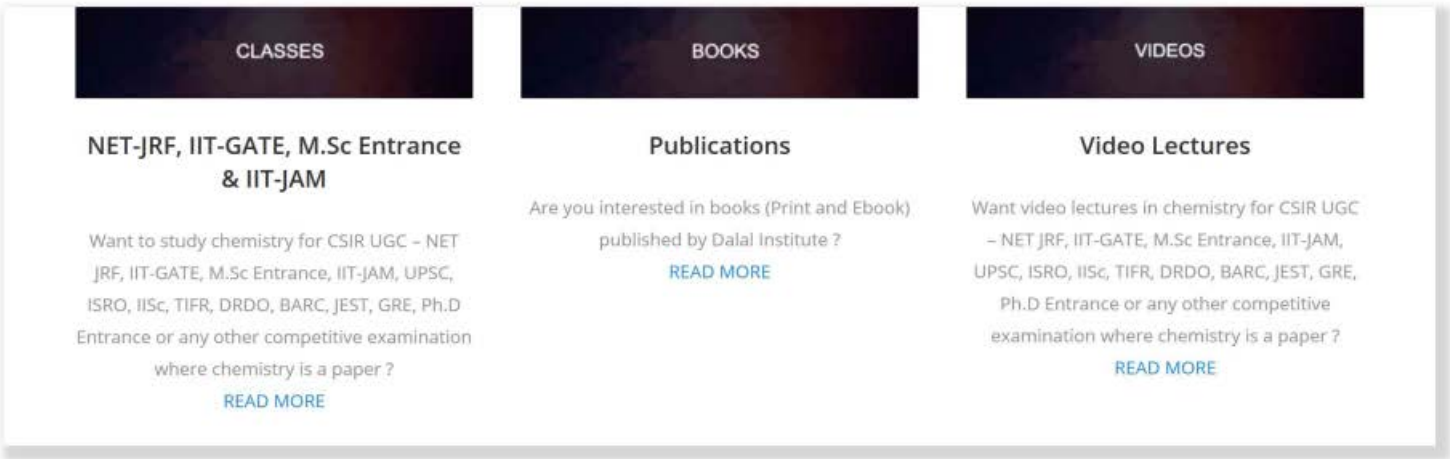

Home: https://www.dalalinstitute.com/
Classes: https://www.dalalinstitute.com/classes/
Books: https://www.dalalinstitute.com/books/
Videos: https://www.dalalinstitute.com/videos/
Location: https://www.dalalinstitute.com/location/
Contact Us: https://www.dalalinstitute.com/contact-us/
About Us: https://www.dalalinstitute.com/about-us/

Postgraduate Level Classes (NET-JRF & IIT-GATE)
Admission
Regular Program Distance Learning
Test Series Result

Undergraduate Level Classes (M.Sc Entrance & IIT-JAM)
Admission
Regular Program Distance Learning
Test Series Result

A Textbook of Inorganic Chemistry – Volume 1

"A Textbook of Inorganic Chemistry – Volume 1 by Mandeep Dalal" is now available globally; including India, America and most of the European continent. Please ask at your local bookshop or get it online here.
READ MORE

International Edition

A TEXTBOOK OF INORGANIC CHEMISTRY

Volume I

MANDEEP DALAL

First Edition

DALAL INSTITUTE

Table of Contents

Mandeep Dalal
(M.Sc, Ph.D, CSIR UGC - NET JRF, IIT - GATE)
Founder & Director, Dalal Institute
Contact No: +91-9802825820
Homepage: www.mandeepdalal.com
E-Mail: dr.mandeep.dalal@gmail.com

Mandeep Dalal is an Indian research scholar who is primarily working in the field of Science and Philosophy. He received his Ph.D in Chemistry from Maharshi Dayanand University, Rohtak, in 2018. He is also the Founder and Director of "Dalal Institute", an India-based educational organization which is trying to revolutionize the mode of higher education in Chemistry across the globe. He has published more than 40 research papers in various international scientific journals, including mostly from Elsevier (USA), IOP (UK) and Springer (Netherlands) .

Other Books by the Author

A TEXTBOOK OF INORGANIC CHEMISTRY - VOLUME I, II, III, IV

A TEXTBOOK OF PHYSICAL CHEMISTRY - VOLUME I, II, III, IV

A TEXTBOOK OF ORGANIC CHEMISTRY - VOLUME I, II, III, IV

ISBN: 978-81-938720-0-0

MRP: Rs 800.00

DALAL INSTITUTE

Main Market, Sector 14, Rohtak, Haryana 124001, India
(+91-9802825820, info@dalalinstitute.com)
www.dalalinstitute.com